

CYCLOSTATIONARITY-BASED DETECTION AND IDENTIFICATION OF BINARY OFFSET CARRIER -MODULATED SIGNALS

Etienne Thuillier and Jarmo Lundén

Aalto University, School of Electrical Engineering,
 Department of Signal Processing and Acoustics, Espoo, Finland
 Email:{etienne.thuillier, jarmo.lunden}@aalto.fi

ABSTRACT

In this paper, cyclostationarity-based detection and identification of binary offset carrier (BOC)-modulated signals is considered. BOC-modulated signals are widely used in current and next-generation global navigation satellite systems. The cyclostationary properties of the BOC-modulated signals are summarized and distinguishing features are discussed. A multiple hypothesis testing problem is formulated for detecting and identifying the strongest BOC-modulated signal from a multi-signal mixture. Two cyclic detection and identification tests are proposed. Their asymptotic distributions under the null hypothesis, when only noise is present, are established. Simulation results that show the very good detection and identification performance of the proposed algorithms are provided.

Index Terms— Binary offset carrier, cyclostationarity, detection, modulation classification

1. INTRODUCTION

Signal detection and identification algorithms have applications, for example, in wireless communication and radar systems. Signal detection has recently received considerable interest in future wireless communications systems, such as cognitive radio systems, for obtaining awareness about the radio frequency spectrum [1]. Many of the commonly employed wireless communication and radar signals exhibit cyclostationarity. Cyclostationarity in these signals may be, e.g., due to modulation and coding. One of the main benefits of cyclostationarity-based algorithms is that cyclostationary properties can be exploited in distinguishing different signals.

In this paper, we focus on cyclostationarity-based detection and identification of binary offset carrier (BOC) -modulated signals. BOC-modulated signals are widely used in current and next-generation global navigation satellite systems (GNSSs) [2, 3]. The different GNSSs share and operate in many of the same frequency bands. Hence, in general, the received signal in a GNSS frequency band is a mixture of

This work has been supported by the Scientific Advisory Board for Defence.

BOC-modulated signals. We employ cyclostationarity-based detection and identification algorithms with the goal of detecting and identifying the strongest BOC-signal in a signal mixture. These techniques can be used, e.g., in future GNSS receivers to decrease the receiver complexity by reducing the set of potential signals to be used for positioning to only the strongest signals [4].

Cyclostationarity-based signal modulation identification and classification methods have been considered, e.g., in [5–7] and the references therein. However, cyclostationarity-based BOC-modulated signal detection and identification has been considered only in few previous works [4]. In [4], a cyclic spectrum-based identification scheme for BOC-modulated signals is proposed. However, the computational complexity of the proposed scheme is high and the performance at low signal-to-noise ratios (SNRs) is poor.

The contributions of this paper are as follows. We formulate a multiple hypothesis testing problem for detecting and identifying the strongest BOC-modulated signal from a multi-signal mixture. We summarize the second-order cyclostationary properties of BOC-modulated signals and identify double the subcarrier frequency as a potential feature for identifying the strongest BOC-modulated signal. We propose two cyclostationarity-based tests for signal detection and identification. Moreover, we establish the asymptotic distributions of the proposed test statistics under the null hypothesis. We provide simulation results showing the very good detection and identification performance of the proposed algorithms.

2. PROBLEM FORMULATION

In this paper, we consider a scenario in which a mixture of different BOC-modulated signals is received. The goal is to detect and identify the strongest signal in the mixture. This can be formulated as a multiple hypothesis testing problem:

$$\begin{aligned} H_0 : \quad & x(k) = w(k) \\ H_i : \quad & x(k) = \sum_{i=1}^d A_i s_{\alpha_i}(k) + w(k), \quad |A_i| \geq |A_j|, \quad \forall j, \quad (1) \\ & i = 1, \dots, d, \end{aligned}$$

where $x(k)$ denotes the received signal, $w(k)$ denotes independent and identically distributed complex noise, s_{α_i} , $\alpha_i \in \mathcal{A}$, denote the zero-mean unit variance candidate signals, and A_i denote their respective amplitudes.

3. BOC-MODULATED SIGNALS

A BOC-modulated signal can be expressed as [3]

$$s(t) = \sum_{n=-\infty}^{\infty} \sum_{k=0}^{N_c-1} b_n c_{n,k} g(t - nT_s - kT_c), \quad (2)$$

where b_n is the n th data symbol, c_k is the k th chip of the spreading code, N_c is the length of the spreading codes, T_c is the chip period, $T_s = N_c T_c$ is the symbol period, and $g(t)$ is a double BOC (DBOC) waveform given by

$$g(t) = \sum_{i=0}^{N_1-1} \sum_{k=0}^{N_2-1} (-1)^{i+k} q\left(t - i \frac{T_c}{N_1} - k \frac{T_c}{N_1 N_2}\right), \quad (3)$$

where $N_1 = 2 \frac{f_{sc}}{f_c}$ is the BOC-modulation order, f_{sc} is the subcarrier frequency, $f_c = \frac{1}{T_c}$, and $q(t)$ is a rectangular pulse shape of unit amplitude and duration equal to $\frac{T_c}{N_1 N_2}$. Different BOC-waveforms are obtained as follows [3]: $N_1 = 1$ and $N_2 = 1$ for BPSK, $N_1 > 1$ and $N_2 = 1$ for SinBOC, and $N_1 > 1$ and $N_2 = 2$ for CosBOC.

3.1. Cyclostationary properties

Assuming that b_n are independent and identically distributed (i.i.d.) and the spreading code $c_{n,k}$ is the same for each data symbol, i.e., $c_{n,k} = c_k$, $\forall n$, the (conjugate) cyclic autocorrelation function of $s(t)$ is given by [4]

$$R_{ss^{(*)}}^{\alpha}(\tau) = \frac{R_{bb^{(*)}}}{T_s} \delta_{((\alpha T_s) \bmod 1)} r_{gg^{(*)}}^{\alpha}(\tau) \otimes \gamma_{cc^{(*)}}^{\alpha}(\tau), \quad (4)$$

where \otimes denotes convolution, $\delta_{((\alpha T_s) \bmod 1)}$ is the Kronecker delta function having value 1 when $\alpha = k/T_s$, $k \in \mathbb{Z}$, and 0 otherwise, and

$$R_{bb^{(*)}} = \lim_{N \rightarrow \infty} \frac{1}{2N+1} \sum_{n=-N}^N b_n b_n^{(*)}, \quad (5)$$

$$\gamma_{cc^{(*)}}^{\alpha}(\tau) = \sum_{n_1=0}^{N_c-1} \sum_{n_2=0}^{N_c-1} c_{n_1} c_{n_2}^{(*)} e^{-j2\pi\alpha n_2 T_c} \delta(\tau - (n_1 - n_2) T_c), \quad (6)$$

$$\begin{aligned} r_{gg^{(*)}}^{\alpha}(\tau) &= g(\tau) \otimes [g^{(*)}(-\tau) e^{j2\pi\alpha\tau}] \\ &= \int_{\mathbb{R}} g(t + \tau) g^{(*)}(t) e^{-j2\pi\alpha t} dt, \end{aligned} \quad (7)$$

and the (conjugate) cyclic spectrum of $s(t)$ is given by [4]

$$\begin{aligned} S_{ss^{(*)}}^{\alpha}(f) &= \frac{R_{bb^{(*)}}}{T_s} \delta_{((\alpha T_s) \bmod 1)} G(f) G^{(*)}((-)(\alpha - f)) \\ &\cdot \Gamma_{cc^{(*)}}^{\alpha T_c}(f T_c), \end{aligned} \quad (8)$$

where

$$\begin{aligned} G(f) &= \int_{\mathbb{R}} g(t) e^{-j2\pi f t} dt, \\ &= T_B \operatorname{sinc}\left(f \frac{T_B}{N_2}\right) \left(\frac{1 - (-1)^{N_2} e^{-j2\pi f T_B}}{1 + e^{-j2\pi f T_B}} \right) \\ &\cdot \left(\frac{1 - (-1)^{N_1} e^{-j2\pi f T_c}}{1 + e^{-j2\pi f T_B}} \right) e^{-j2\pi f \frac{T_B}{N_2}}, \end{aligned} \quad (9)$$

$$\Gamma_{cc^{(*)}}^{\beta}(\nu) = \mathcal{C}(\nu) \mathcal{C}^{(*)}((-)(\beta - \nu)), \quad (10)$$

$$\mathcal{C}(\nu) = \sum_{n=0}^{N_c-1} c_n e^{-j2\pi\nu n}, \quad (11)$$

where $T_B = \frac{T_c}{N_1}$ and $\operatorname{sinc}(x) = \frac{\sin(\pi x)}{\pi x}$.

BOC-modulated signals are, thus, cyclostationary at cycle frequencies $\alpha = k/T_s$, $k \in \mathbb{Z}$. In the following, we will use double the subcarrier frequency $\alpha = 2f_{sc} = N_1/T_c = N_1 N_c / T_s = 1/T_B$ to identify the strongest BOC-modulated signal. Double the subcarrier frequency is the strongest non-zero conjugate cycle frequency and thus could allow identifying the correct BOC-modulation provided that the subcarrier frequencies among the potential signals are distinct, even if the signals have overlapping cycle frequencies.

It is to be noted that the real-life signals used in GNSSs are somewhat more complicated than the model employed above. E.g., a more accurate cyclic spectral analysis of the real-life GPS-L1 signal can be found in [8]. However, here our aim is to perform a preliminary analysis with general BOC-models without focusing too much on particular systems.

4. CYCLOSTATIONARITY-BASED DETECTION AND IDENTIFICATION

We define the cyclostationarity-based detection and identification statistic over a set of candidate signals $s_{\alpha}(k)$, $\alpha \in \mathcal{A}$, each associated with a distinct non-zero cycle frequency α , as

$$Z_{(*)} = \max_{\alpha \in \mathcal{A}} \frac{M \hat{N}_0^{-2}}{\sum_{\tau \in \mathcal{T}} |R_{s_{\alpha} s_{\alpha}^{(*)}}^{\alpha}(\tau)|^2} \left| \sum_{\tau \in \mathcal{T}} R_{s_{\alpha} s_{\alpha}^{(*)}}^{\alpha}(\tau)^* \hat{R}_{xx^{(*)}}^{\alpha}(\tau) \right|^2, \quad (12)$$

where M is the number of observations, \mathcal{T} is a set of time lags, $R_{s_{\alpha} s_{\alpha}^{(*)}}^{\alpha}(\cdot)$ denotes the (conjugate) cyclic autocorrelation function of a candidate signal $s_{\alpha}(k)$ defined by

$$R_{s_{\alpha} s_{\alpha}^{(*)}}^{\alpha}(\tau) = \lim_{L \rightarrow \infty} \frac{1}{2L+1} \sum_{k=-L}^L E[s_{\alpha}(k+\tau) s_{\alpha}^{(*)}(k)] e^{-j2\pi\alpha k}, \quad (13)$$

$\hat{R}_{xx^{(*)}}^{\alpha}(\tau)$ is the estimate of the (conjugate) cyclic autocorrelation function of the received signal $x(k)$ defined by

$$\hat{R}_{xx^{(*)}}^{\alpha}(\tau) = \frac{1}{M} \sum_{k=1}^M x(k+\tau) x^{(*)}(k) e^{-j2\pi\alpha k}, \quad (14)$$

and \hat{N}_0 is the estimate of the noise variance defined by

$$\hat{N}_0 = \frac{1}{M} \sum_{k=1}^M |x(k)|^2, \quad (15)$$

where it has been assumed that $x(k)$ is zero-mean.

Detection is declared if the test statistic exceeds a predefined threshold, i.e.,

$$Z_{(*)} \stackrel{H_i}{\gtrless}_{H_0} \lambda, \quad (16)$$

where the threshold λ is selected such that the detection false alarm rate $p(Z_{(*)} > \lambda | H_0) = p_{fa}$, where p_{fa} is the desired false alarm rate. Further, if a detection occurs, a candidate signal is elected among the set of candidate signals such that the elected candidate's cycle frequency α maximizes $Z_{(*)}$.

If the true (conjugate) cyclic autocorrelations $R_{s_\alpha s_\alpha^{(*)}}^\alpha(\tau)$ of the candidate signals $s_\alpha(k)$, $\alpha \in \mathcal{A}$, are unknown but the cycle frequencies α are known, we employ the following test:

$$W_{(*)} = \max_{\alpha \in \mathcal{A}} M \hat{N}_0^{-2} \sum_{\tau \in \mathcal{T}} \left| \hat{R}_{xx^{(*)}}^\alpha(\tau) \right|^2 \stackrel{H_i}{\gtrless}_{H_0} \gamma, \quad (17)$$

where γ is the test threshold selected such that the detection false alarm rate $p(W_{(*)} > \gamma | H_0) = p_{fa}$.

4.1. Asymptotic distributions of the test statistics

Under some general assumptions, the (conjugate) cyclic autocorrelation estimator is asymptotically complex Normal distributed [9, Theorem 6.4]: for every fixed α_i and τ_i , $i = 1, \dots, n$, the random variables

$$V_i = \sqrt{M} \left[\hat{R}_{xx^{(*)}}^{\alpha_i}(\tau_i) - R_{xx^{(*)}}^{\alpha_i}(\tau_i) \right] \quad (18)$$

are asymptotically ($M \rightarrow \infty$) jointly complex Normal with asymptotic covariance matrix Σ and asymptotic conjugate covariance matrix C with entries, respectively, given by:

$$\Sigma_{ik} = \lim_{M \rightarrow \infty} \text{Cov}\{V_i, V_k\} = S_{x_{\tau_i} x^{(*)} x_{\tau_j}^{*(*)}}^{\alpha_i - \alpha_k}(-\alpha_k) \quad (19)$$

$$C_{ik} = \lim_{M \rightarrow \infty} \text{Cov}\{V_i, V_k^*\} = S_{x_{\tau_i} x^{(*)} x_{\tau_j}^{*(*)}}^{\alpha_i + \alpha_k}(\alpha_k), \quad (20)$$

where $S_{x_{\tau_i} x^{(*)} x_{\tau_j}^{*(*)}}^\alpha(f)$ and $S_{x_{\tau_i} x^{(*)} x_{\tau_j}^{*(*)}}^{\alpha}(f)$ denote the cyclic spectrum and the conjugate cyclic spectrum of $y^{(*)}(k; \tau) = x(k + \tau)x^{(*)}(k)$, respectively. The cyclic spectrum is defined by

$$\begin{aligned} S_{x_{\tau} x^{(*)} x_{\rho}^{*(*)}}^\alpha(f) = & \\ & \lim_{M \rightarrow \infty} \frac{1}{2M+1} \sum_{k=-M}^M \sum_{\xi=-\infty}^{\infty} \text{cum}\{y^{(*)}(k; \tau), y^{*(*)}(k + \xi; \rho)\} \\ & \cdot e^{-j2\pi f \xi} e^{-j2\pi \alpha k}, \end{aligned} \quad (21)$$

and the conjugate cyclic spectrum is defined by

$$\begin{aligned} S_{x_{\tau} x^{(*)} x_{\rho} x^{(*)}}^\alpha(f) = & \\ & \lim_{M \rightarrow \infty} \frac{1}{2M+1} \sum_{k=-M}^M \sum_{\xi=-\infty}^{\infty} \text{cum}\{y^{(*)}(k; \tau), y^{(*)}(k + \xi; \rho)\} \\ & \cdot e^{-j2\pi f \xi} e^{-j2\pi \alpha k}. \end{aligned} \quad (22)$$

Under the null hypothesis, the mean of the (conjugate) cyclic autocorrelation estimator $\hat{R}_{xx^{(*)}}^\alpha(\tau)$ is zero, $\forall \tau$ and $\forall \alpha \neq 0$, and the asymptotic covariance of $r_i = \sum_{\tau \in \mathcal{T}} R_{s_{\alpha_i} s_{\alpha_i}^{(*)}}^{\alpha_i}(\tau)^* \hat{R}_{xx^{(*)}}^{\alpha_i}(\tau)$ is given by

$$\Sigma_{r_i r_k} | H_0 = \begin{cases} \sum_{\tau \in \mathcal{T}} |R_{s_{\alpha_i} s_{\alpha_i}^{(*)}}^{\alpha_i}(\tau)|^2 S_{x_{\tau} x^{(*)} x_{\tau}^{*(*)}}^0(0), & i = k \\ 0, & i \neq k, \end{cases} \quad (23)$$

where $S_{x_{\tau} x^{(*)} x_{\tau}^{*(*)}}^0(0)$ is estimated as $\hat{S}_{x_{\tau} x^{(*)} x_{\tau}^{*(*)}}^0(0) = \hat{N}_0^2$ with \hat{N}_0 given by (15).

Furthermore, the asymptotic conjugate covariance of r_i and r_k is under the null hypothesis equivalent to zero, i.e.,

$$C_{r_i r_k} | H_0 = 0, \quad \forall i, k. \quad (24)$$

Consequently, it follows that $Z_{(*)}$ is under the null hypothesis a maximum of independent chi-square distributed random variables with one complex degree of freedom and $W_{(*)}$ is a maximum of independent chi-square distributed random variables with $|\mathcal{T}|$ complex degrees of freedom where $|\cdot|$ denotes the cardinality of a set. The cumulative distribution function of the maximum of d independent chi-square distributed random variables with N complex degrees of freedom is given by

$$F(x) = \left(\frac{\gamma(N, x)}{\Gamma(N)} \right)^d, \quad (25)$$

where $\gamma(N, x) = \int_0^x t^{N-1} e^{-t} dt$ is the lower incomplete gamma function and $\Gamma(N) = (N-1)!$. In the above tests, we have $d = |\mathcal{A}|$.

5. SIMULATION RESULTS

In this section, we illustrate the performance of the proposed cyclostationarity-based detection and identification scheme with different BOC signal mixtures in additive white Gaussian noise (AWGN) channels. We define the SNR in dB as $\text{SNR}_{dB} = 10 \log_{10} \frac{\max_i |A_i|^2}{\sigma_w^2}$, where σ_w^2 denotes the noise variance.

Fig. 1 illustrates that the established asymptotic distributions match accurately the empirical distributions under H_0 in AWGN. The empirical curves have been obtained from 10000 independent experiments. The number of observations is 10000, the number of time lags is 20, and the number of potential systems (different cycle frequencies) is 12.

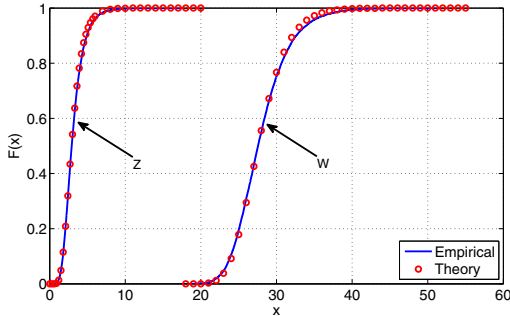


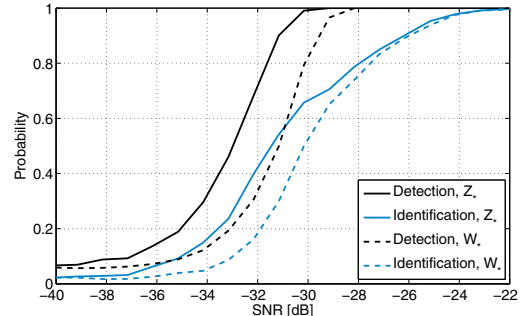
Fig. 1. The empirical cumulative distribution functions (CDFs) of the test statistics in (12) and (17) vs. the theoretical asymptotic CDFs under H_0 in AWGN.

In the first identification experiment, we consider a mixture of three BOC-modulated signals: SinBOC(10,5), SinBOC(15,2.5), and SinBOC(14,2), where SinBOC(m,n) denotes a SinBOC-waveform with subcarrier frequency $f_{sc} = m f_{ref}$ and chip frequency $f_c = n f_{ref}$, where $f_{ref} = 1.023$ MHz. These are examples of BOC-waveforms proposed for GPS, Galileo, and BeiDou. The spreading sequences are Gold-codes of length 31. The goal is to detect and identify the strongest signal in the mixture. The identification system classifies a detected signal to three classes corresponding to the cycle frequencies equivalent to double the subcarrier frequencies of the three candidate waveforms. The sampling frequency is $64f_{ref}$ and the observation period is 0.1s. The set of time lags used by the algorithms is $\mathcal{T} = \{\pm 1, \pm 2, \pm 3, \pm 4\}$.

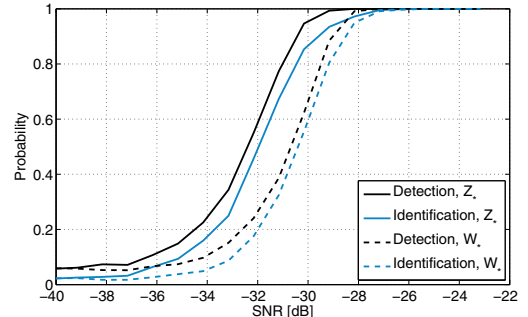
Fig. 2 depicts the performance of the proposed detection and identification scheme as a function of the SNR. The curves are averages over 1500 independent simulations. It can be seen that exploiting the knowledge of the true cyclic autocorrelation improves both the detection and identification performance, i.e., test statistic Z_* outperforms test statistic W_* in all cases. When the power differences among the signals are larger (b) the probability of correct identification is very close to the probability of detection. With smaller power differences among the signals (a) there is more confusion between the signal classes and thus identification requires considerably higher SNR to achieve accuracy comparable to the detection accuracy.

Table 1 shows the confusion matrices for the proposed identification schemes at SNR of -29 dB. For the test statistic Z_* the identification performances for the different signal classes are very similar. In comparison, with the test statistic W_* SinBOC(14,2)-modulated signals are clearly the easiest to identify.

Next, we consider another mixture of three signals: SinBOC(2,1), SinBOC(3,1), and SinBOC(4,1). This is at least in theory a harder signal mixture to correctly identify since all of the signals share the same symbol and chip frequen-



(a) 1 dB power difference



(b) 3 dB power difference

Fig. 2. Probabilities of detection and correct identification of the strongest signal in a mixture of SinBOC(10,5), SinBOC(15,2.5), and SinBOC(14,2) modulated signals vs. SNR in AWGN for a false alarm rate of 0.05. The power differences among the signals are (a) 1 dB and (b) 3 dB.

cies. Hence, all of their cycle frequencies are overlapping which is not the case in the former scenario. The sampling frequency is in this case $48f_{ref}$ and the potential number of classes is 12, i.e., SinBOC($m,1$), $m = 1, 2, \dots, 12$. Consequently, there are more potential classes (although the number of signals is three and the signal classes are the same in each simulation) which makes the identification harder. The set of time lags used by the algorithms is $\mathcal{T} = \{\pm 1, \pm 2, \dots, \pm 10\}$. The other simulation parameters are the same as earlier.

Fig. 3 shows the detection and identification performance of the proposed schemes as a function of the SNR in AWGN. The false alarm rate parameter is 0.05. The curves are averages over 1500 independent simulations. When the power differences among the signals (b) are large the correct identification performance is very close to the detection performance. Consequently, increasing the number of potential classes does not appear to deteriorate the identification performance in this case. However, when the power of the mixture components are closer to each other (a) the identification performance degrades significantly. That is, SinBOC(2,1)- and SinBOC(3,1)-modulated signals are incorrectly identified as SinBOC(4,1)-modulated signals even at moderately high SNRs.

Table 1. Confusion matrices for identifying the strongest signal in a three signal mixture of SinBOC(10,5), SinBOC(15,2.5), and SinBOC(14,2) modulated signals at SNR of -29 dB in AWGN. The strongest signal power is 3 and 6 dB higher than the second and third strongest signal powers, respectively.

Algorithm	Signal class	SinBOC(10,5)	SinBOC(15,2.5)	SinBOC(14,2)	no detection
Z_*	SinBOC(10,5)	0.922	0.032	0.032	0.014
	SinBOC(15,2.5)	0.010	0.946	0.040	0.004
	SinBOC(14,2)	0.054	0.008	0.936	0.002
W_*	SinBOC(10,5)	0.774	0.040	0.038	0.148
	SinBOC(15,2.5)	0.016	0.784	0.050	0.150
	SinBOC(14,2)	0.079	0.016	0.853	0.052

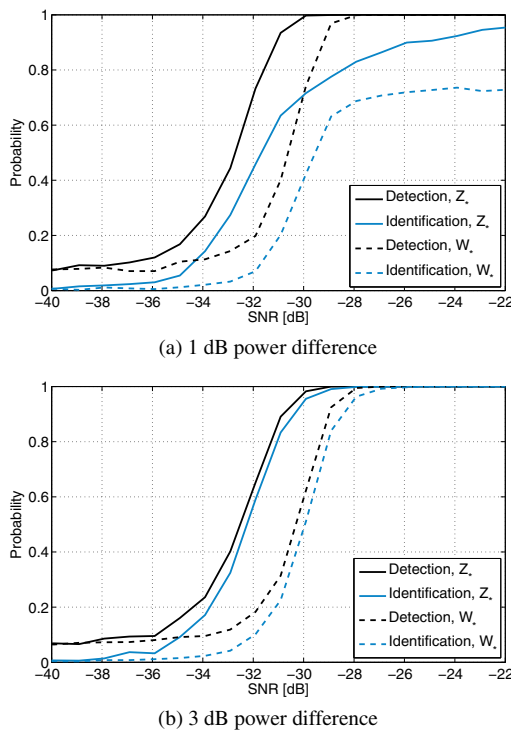


Fig. 3. Probabilities of detection and correct identification of the strongest signal in a mixture of SinBOC(2,1), SinBOC(3,1), and SinBOC(4,1) modulated signals vs. SNR in AWGN for a false alarm rate of 0.05. The power differences among the signals are (a) 1 dB and (b) 3 dB.

6. CONCLUSION

In this paper, cyclostationarity-based detection and identification of BOC-modulated signals has been considered. The goal has been to detect and identify the strongest BOC-modulated signal from a multi-signal mixture. We have identified double the subcarrier frequency as a potential cyclic feature and proposed two cyclostationarity-based detection and identification tests. Furthermore, we have established the asymptotic distributions of the proposed test statistics under the null hypothesis. Our simulation results show that the proposed algorithms have very good detection and identification

performance even at very low SNRs.

REFERENCES

- [1] E. Biglieri, A. Goldsmith, L. Greenstein, N. Mandayam, and H.V. Poor, *Principles of Cognitive Radio*, Cambridge, UK: Cambridge University Press, 2013.
- [2] J. W. Betz, “Binary offset carrier modulations for radionavigation,” *Navigation*, vol. 48, no. 4, pp. 227–245, Mar. 2001.
- [3] E. S. Lohan, A. Lakhzouri, and M. Renfors, “Binary-offset-carrier modulation techniques with applications in satellite navigation systems,” *Wireless Commun. Mobile Comput.*, vol. 6, no. 5, pp. 767–779, Aug. 2007.
- [4] E. S. Lohan, J. Lundén, G. Seco-Granados, J. A. López-Salcedo, and V. Koivunen, “Cyclic frequencies of BOC-modulated GNSS signals and their potential within a cognitive positioning framework,” *Navigation*, vol. 61, no. 2, pp. 95–114, Summer 2014.
- [5] C. M. Spooner, “Classification of co-channel communication signals using cyclic cumulants,” in *Proc. 29th Asilomar Conference on Signals, Systems and Computers*, Pacific Grove, CA, USA, Oct. 30–Nov. 1, 1995, vol. 1, pp. 531–536.
- [6] O. A. Dobre, A. Abdi, Y. Bar-Ness, and W. Su, “Cyclostationarity-based modulation classification of linear digital modulations in flat fading channels,” *Wireless Pers. Commun.*, vol. 54, no. 4, pp. 699–717, Sep. 2010.
- [7] O. A. Dobre and R. Inkol, “Blind signal identification: Achievements, trends, and challenges,” in *Proc. 9th International Conference on Communications (COMM)*, Bucharest, Romania, Jun. 21–23, 2012, pp. 349–352.
- [8] A. Napolitano and I. Perna, “Cyclic spectral analysis of the GPS signal,” *Digit. Signal Process.*, vol. 33, pp. 13–33, Oct. 2014.
- [9] A. Napolitano, “Discrete-time estimation of second-order statistics of generalized almost-cyclostationary processes,” *IEEE Trans. Signal Process.*, vol. 57, no. 5, pp. 1670–1688, May 2009.